

Artificial Cells, Nanomedicine, and Biotechnology

An International Journal

ISSN: (Print) (Online) Journal homepage: informahealthcare.com/journals/ianb20

Layered double hydroxide nanoparticles as an appealing nanoparticle in gene/plasmid and drug delivery system in C2C12 myoblast cells

Parivar Yazdani, Elham Mansouri, Shirin Eyvazi, Vahid Yousefi, Homan Kahroba, Mohammad Saeid Hejazi, Asghar Mesbahi, Vahideh Tarhriz & Mir Mahdi Abolghasemi

To cite this article: Parivar Yazdani, Elham Mansouri, Shirin Eyvazi, Vahid Yousefi, Homan Kahroba, Mohammad Saeid Hejazi, Asghar Mesbahi, Vahideh Tarhriz & Mir Mahdi Abolghasemi (2019) Layered double hydroxide nanoparticles as an appealing nanoparticle in gene/plasmid and drug delivery system in C2C12 myoblast cells, *Artificial Cells, Nanomedicine, and Biotechnology*, 47:1, 436-442, DOI: [10.1080/21691401.2018.1559182](https://doi.org/10.1080/21691401.2018.1559182)

To link to this article: <https://doi.org/10.1080/21691401.2018.1559182>



© 2019 The Author(s). Published by Informa UK Limited, trading as Taylor & Francis Group.



Published online: 01 Feb 2019.



[Submit your article to this journal](#)



Article views: 3913



[View related articles](#)




[View Crossmark data](#)



Citing articles: 20 [View citing articles](#)

Layered double hydroxide nanoparticles as an appealing nanoparticle in gene/plasmid and drug delivery system in C2C12 myoblast cells

Parivar Yazdani^a, Elham Mansouri^a, Shirin Eyvazi^b, Vahid Yousefi^a , Homan Kahroba^c,
Mohammad Saeid Hejazi^{a,c,d}, Asghar Mesbahi^a, Vahideh Tarhriz^a and Mir Mahdi Abolghasemi^e

^aMolecular Medicine Research Center, Biomedicine Institute, Tabriz University of Medical Sciences, Tabriz, Iran; ^bDepartment of Biotechnology, School of Advanced Technologies in Medicine, Shahid Beheshti University of Medical Sciences, Tehran, Iran; ^cDepartment of Molecular Medicine, Faculty of Advanced Medical Sciences, Tabriz University of Medical Sciences, Tabriz, Iran; ^dFaculty of Pharmacy, Tabriz University of Medical Sciences, Tabriz, Iran; ^eDepartment of Chemistry, Faculty of Science, University of Maragheh, Maragheh, Iran

ABSTRACT

Gene and drug delivery systems need crucial update in the issue of nanocarriers. Layered double hydroxides (LDHs) are known as biocompatible inorganic lamellar nanomaterials with versatile properties. In the present study, Zn/Al-LDH nanoparticle was synthesized and characterized by FTIR, XRD, SEM, TEM and Zeta potential tests and then intercalated with valproate and methyldopa by co-precipitation and ion exchange methods. These nanocarriers were applied as high activity nanolayers-based delivery systems. On the other hand, Zn/Al-LDH + plasmid/gene (pCEP4/Cdk9) evaluated on C2C12 myoblast cells. Co-operation loading indicated high efficiency of sorting and release of drugs. Additionally, the Real-Time PCR and Western blotting results for plasmid-gene (pCEP4/Cdk9) delivery showed that Zn/Al-LDH nanoparticles can be used as an effective carrier in cellular uptake and release of genes for gene therapy. Easy and cost-effective production of Zn/Al-LDH nanoparticles proposed them as potential alternatives for the traditional routs of drug/gene delivery.

ARTICLE HISTORY

Received 26 October 2018
Revised 25 November 2018
Accepted 27 November 2018



KEYWORDS


Layered double hydroxide;
nanomaterial; drug/gene
delivery; pCEP4/Cdk9

Introduction

Layered double hydroxides (LDHs) are known as biocompatible inorganic lamellar nanomaterials with versatile properties which make them appealing nanocarriers [1]. Two-dimensional (2D) layered nanostructures provide preservative transferring for their cargos due to physicochemical properties with timely release [2]. The intercalating properties of layered nanostructures support them as an emerging carrier to develop hybrid materials at nanoscale dimensions (nanocomposites). Preserver molecules like LDHs protect the sorted drugs from environmental damage, degradation and alternation beside enhancement of their loading density, physicochemical stability, and penetration ability. LDHs stabilize the drugs and biomolecules within the interlayer of carriers by infiltration into the cells, for example magnesium and aluminium-rich LDHs support cargoes form anti-acid and anti-pepsin agents, respectively. LDHs unique structural characteristics including cationic layers, exchangeable interlayer anions, and high zeta potential potent them for preserving loaded molecules [1,3–5]. LDHs derived from brucite are positively charged and easily attach to the negatively charged cell walls to enhance intercalation and transferring efficiency of loaded drugs/genes [6,7].

Ease of LDHs synthesizing beside controllable anionic exchange capacity and anion capture ability with the high surface functionality facilitates their interlayer loading of biomolecules [8–12]. The capability of targeted delivery and controllable release of LDHs excel them in contrast to systematic drug delivery system by reduction of misplaced drug delivery to promote potential side effects. Timely drug release of LDHs introduced them as reliable drug delivery vectors with a suitable half-life of drug release in comparison to other layered nanomaterials. LDHs decrease drug dissolution rate in aquatic environments by delaying drug dissolution to vectorize the drugs into the targeted location of activity [13]. Many studies have investigated the efficacy of LDHs as a gene, vitamin, anticancer, anti-inflammatory, and pharmacologically active drugs delivery systems [14–18]. Some of LDHs such as Mg/Al, Zn/Al, and Fe/Al can appear as excellent candidates as drug/gene carriers with controllable release system due to high biocompatibility, ease of synthesis process, stability, tunable particle size, and targeted delivery [19–23]. The valproate and methyldopa have been previously selected as model drugs to intercalate into the Zn/Al-LDH in order to study the release behaviour of LDH-based delivery systems.

CONTACT  Vahideh Tarhriz  t.tarhriz@yahoo.com, tarhrizv@tbzmed.ac.ir  Molecular Medicine Research Center, Biomedicine Institute, Tabriz University of Medical Sciences, Tabriz, 51664-14766, Iran; Mir Mahdi Abolghasemi mehdiabolghasemi@gmail.com Department of Chemistry, Faculty of Science, University of Maragheh, Maragheh, 55181-83111, Iran;

 Supplemental data for this article can be accessed [here](#).

© 2019 The Author(s). Published by Informa UK Limited, trading as Taylor & Francis Group.

This is an Open Access article distributed under the terms of the Creative Commons Attribution License (<http://creativecommons.org/licenses/by/4.0/>), which permits unrestricted use, distribution, and reproduction in any medium, provided the original work is properly cited.

In this study, we focused on the new application of layered double hydroxide nanostructure as a gene/drug delivery. Accordingly, we evaluated LDHs plasmid/gene (pCEP4/Cdk9) cellular uptake ability as an outstanding candidate for cellular delivery of DNA or RNA for suggesting Zn/Al-LDH as an easy and cost-effective synthesizing method and as proper and reliable alternatives to traditional and expensive methods.

Materials and methods

Materials and bio-materials

Zinc chloride ($\text{ZnCl}_2 \cdot 6\text{H}_2\text{O}$), aluminium chloride ($\text{AlCl}_3 \cdot 9\text{H}_2\text{O}$), sodium hydroxide (NaOH), methanol, 3-(4,5-dimethylthiazol-2-yl)-2,5-diphenyltetrazolium bromide, DMSO (Dimethyl sulfoxide), agar-agar, Tris-base (2-Amino-2-hydroxymethyl-propane-1,3-diol), SDS (Sodium Dodecyl Sulfate), and Agarose were purchased from Merck Hygromycin B was purchased from Roche; Sorenson Glycine Buffer (containing glycine and sodium chloride), methyl dopa 50 mg/ml (M1500000- Sigma-Aldrich), and Valproate 100 mg/ml (V0033000) were obtained from Sigma-Aldrich. Anti-Cdk9 rabbit polyclonal antibody (H-169, sc-8338) and goat anti-rabbit-HRP conjugated anti-body were prepared from Santa Cruz Biotechnology. All chemical solvents were obtained from the Sigma or Merck companies. The pCEP4/Cdk9 plasmid expressing full-length wild-type Cdk9 has been constructed in our recent research [24].

Escherichia coli O157 PTCC 1276 and *Streptococcus aureus* ATCC were obtained from Iranian Biological Research Center, and C2C12 myoblast cells were purchased from the National Cell Bank of Iran (Pasteur Institute, Iran).

Apparatus

Powder X-ray diffraction (PXRD) patterns were obtained through a Siemens D-5005 model diffractometer using $\text{CuK}\alpha$ ($\lambda = 0.15418 \text{ nm}$) radiation at 40 kV and 80 mA [25]. The morphologies of the products were observed using a Vega-Tescan model scanning electron microscope (Vega-Tescan) and Philips CM30 transmission electron microscope (TEM). Fourier-transform infrared spectroscopy (FTIR) spectra were obtained using PerkinElmer, Waltham, USA. The LDH suspension was examined with PCS (Nanosizer Nano ZS, Malvern Instruments) to determine the Zeta potential [26].

Synthesis of Zn/Al-LDHs

Zn-Al layered double hydroxides were synthesized by a coprecipitation method at a constant pH of 9 of the solution. 2.1 g of $\text{ZnCl}_2 \cdot 6\text{H}_2\text{O}$ and 0.72 g of $\text{AlCl}_3 \cdot 9\text{H}_2\text{O}$ dissolved in 30 ml of deionized water, mixed at room temperature, and 120 ml of 0.15 M NaOH solution were added dropwise under a nitrogen atmosphere. The obtained slurry was hydrothermally aged at 80°C for 24 h to promote the complete growth of the nanoparticles crystals; after filtration, it was washed repeatedly with deionized water, and finally, the white powder of Zn-Al was dried at 60°C for 24 h [27].

Antibacterial and cytotoxicity assays

MTT assay was carried out to measure both the antibacterial activity and cytotoxicity of the nanomaterials. The antibacterial activity was evaluated by the micro-dilution assay against *Escherichia coli* O157 PTCC 1276 and *Streptococcus aureus* ATCC as the human pathogenic organisms in different concentrations of Zn/Al-LDH (0, 50, 100, 150, 200 and 250 of $\mu\text{g mL}^{-1}$). To measure cell viability, growing myoblast C2C12 cells were seeded at a density of 0.5×10^4 cells per well in 200 ml of growth medium with three particle sizes (5–10, 100–200, and 200–300 nm) and two different concentrations (0.001 and 0.005 g) in 96 well plates. After incubation for 48 h, the media was replaced with fresh culture media containing MTT solution (0.5 mg/ml), and the cells were incubated for an additional 4 h at 37°C . The absorbance was measured at 570 nm using a spectrophotometric microplate reader (Biotek, EL x800.) [24].

Loading and release examination of valproate and methyl dopa

In the first stage, 1.8 g of zinc chloride, 0.72 g aluminium chloride, and 0.6 g each of the drugs (methyl dopa and valproate) were solvated in 30 ml of deionized water. Afterwards, 120 ml of 0.15 M NaOH solution was added dropwise and under a nitrogen atmosphere. The mixture was stirred vigorously for 30–40 min. The product was separated by centrifugation and washed three times with deionized water. In the end, the final synthesized product was dissolved in 120 ml of deionized water and allowed to react in the oven for 12 h, and then it was separated by centrifugation and dried.

In the second method of loading, drugs were added to LDH by anion exchange method. Briefly, 0.5 g of Zn/Al-LDH nanoparticle was added to 50 ml of drugs (300 ppm) and stirred for 2 h. After drug loading by exchange method, the mixture was filtered and dried. The drug release examinations were performed at room temperature by a rotary shaker at 90 rpm. 0.1 g of loaded LDH sample was placed into 20 ml of a pH = 7.4 phosphate-citrate and HCl buffer. 5 ml of the solution was withdrawn at predetermined time intervals and replaced with 5 ml of fresh buffer. The absorbance was measured at $\lambda = 205 \text{ nm}$ and $\lambda = 280 \text{ nm}$ via double ray spectrophotometer to obtain a fix absorption number. Afterwards, absorption diagram of the released drug in predetermined wavelength was plotted.

RNA extraction and quantitative real-time PCR

The total RNA was extracted from the transfected and control cells using RNX-Plus reagent (Cinnagen, Co. Tehran, Iran) according to the manufacturer's protocol. 0.5 μg RNA samples were reverse transcribed into the cDNA using random hexamer primers and MLV reverse transcriptase (PrimeScriptTM RT Reagent Kit, RR037Q, TaKaRa). Quantitative PCR was performed with the 'SYBR Green I Master Mix' kit (RR820L, Takara) using a Rotor-Gene 6000 instrument (Corbett, Australia). The average threshold (Ct) was determined for

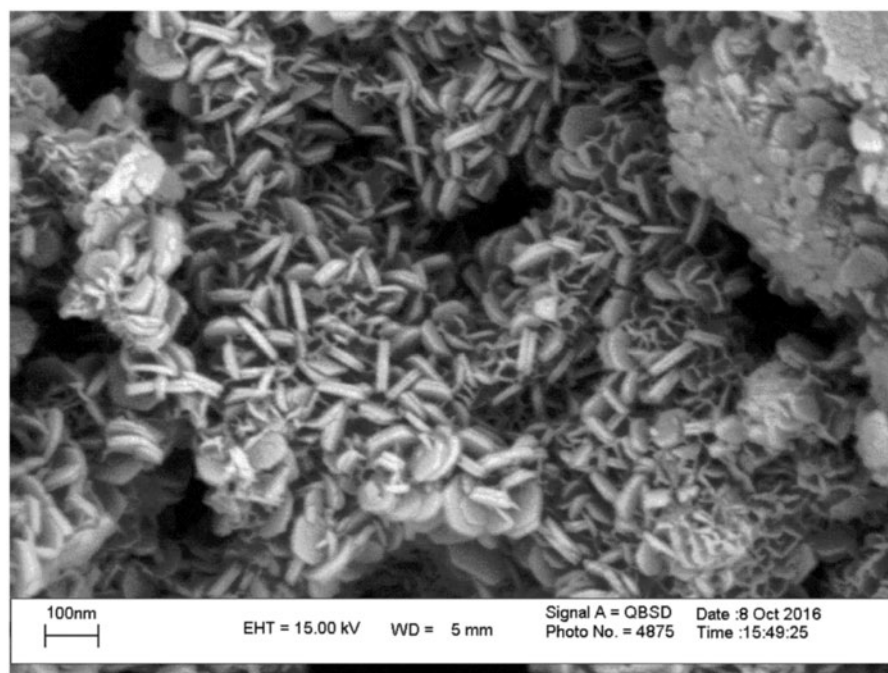


Figure 1. Scanning electron micrograph of Zn/Al-LDH nanoparticles that layered structure of Zn/Al-LDH nanoparticles was obvious.

each gene and normalized to β -actin mRNA level as an internal reference gene. Sequences of primers are provided in Table S1 (Supplementary Table 1).

Western blotting analysis

Total protein lysates of cell cultures were blotted by the following antibodies for immune detection: Anti-Cdk9 rabbit polyclonal antibody rabbit (H-169, sc-8338) in a 1:500 dilution in PBS, 2.5% Blotto, 0.05% Tween-20, mouse monoclonal anti- β -actin (T6199, Sigma) 1:2000, peroxidase-coupled goat anti-rabbit secondary antibody (Santa Cruz Biotechnology) 1:10,000 and peroxidase-coupled rabbit anti-mouse secondary antibody (Santa Cruz Biotechnology) 1:10,000 [24,28].

Statistical analysis

Data were expressed as means \pm SEM. Differences between the two groups were tested using the Mann-Whitney test for nonparametric samples. The p values $< .05$ was considered statistically significant.

Results and discussion

Characterization

Scanning Electron Microscope (SEM) was used for morphology evaluation of the Zn/Al-LDH nanoparticles to confirm the layered structure and size range of the nanoparticles. SEM images (Figure 1) indicated that the structure of Zn/Al-LDH nanoparticles is uniform and homogeneous. Meanwhile, Figure S1 showed the narrow size distribution of Zn/Al-LDH nanoparticles with a mean diameter of ~ 74 nm.

The particle size in the range of 60–80 nm and the layer morphology of the Zn/Al-LDH were indicated by the TEM

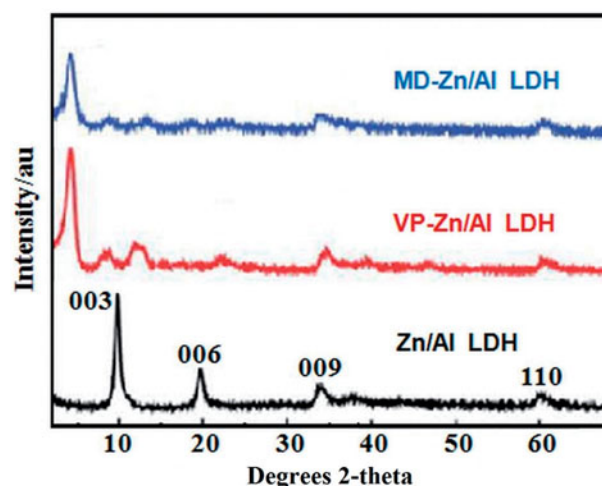


Figure 2. Powder XRD patterns of (a) Zn/Al diffraction peaks distinctive of an LDH structure), (b) VP- Zn/Al-LDH, and (c) MD-Zn/Al-LDH.

micrograph. The measured particle size from the distribution graph was corroborated well with the obtained particle size of Zn/Al-LDH via TEM micrograph (Figure S2).

The XRD pattern of Zn/Al-LDH is shown in the range of $2\theta = 2^\circ - 70^\circ$ in Figure 2. The XRD pattern of the Zn/Al-LDH sample indicates characteristic diffractions of hydrotalcite (PDF: 00-011-0614). The diffraction peaks at $2\theta = 11.64, 20.68, 34.85$ and 61.04 , respectively, correspond to the (003), (006), (009) and (110) of LDH well-crystallized structure. Correspondingly, lamellar and symmetrical structure of 3R rhombic was confirmed. The basal spacing (d_{003}) corresponding to Cl^- ions between the interlayers was expected. The lattice parameters of a and c could be calculated from sever picks of (003), (006) and (110). Figure 2 showed that displacement of the main pick (basal spacing) towards the lower angles indicates main space alternation and valproic acid drug (guest anion)

placement instead of primary anions. Angle reduction expresses an increase in the spacing of the layers.

Moreover, the FT-IR spectra of Zn/AI-LDH, VP-Zn/AI-LDH and MD-Zn/AI-LDH nanoparticles in the $400\text{--}4000\text{ cm}^{-1}$ showed the exhibit basic characteristic peaks at $\sim 451\text{ cm}^{-1}$ that were attributed to the presence of M–O (metal–oxygen group) bonds stretching vibration. The broad peak centred at $\sim 3440\text{ cm}^{-1}$ corresponds to a combination of the stretching vibration of a hydrogen bond between water molecules and metal hydroxyl in the hydroxide groups of the brucite sheets and interlayer water molecules. The absorbance at 1644 cm^{-1} is related to the bending vibrations of the interlayer water molecules. According to Figure 3, the comparison between the FT-IR spectra of VP-Zn/AI-LDH and LDH various spectra groups such as carboxylic acid COOH, C–H and C–C indicates successful loading of the drug into interlayer of LDH. As indicated, the characteristic peaks of 630 cm^{-1} (C–C group) and 2924 cm^{-1} (C–H group) are assigned. The 1373 cm^{-1} and 1514 cm^{-1} spectra are related to symmetrical and asymmetric

stretching vibrations of a carboxylate group, respectively. The interaction between the carboxylate head and the metal atom was considered in four types: monodentate, bridging, chelating, and ionic interaction [29–31]. According to Zhang et al., the wave-number separation, Δ , between the asymmetric and symmetric IR peaks is applicable to distinguish the type of interaction between the carboxylate head and the metal atom. The largest Δ ($200\text{--}320\text{ cm}^{-1}$) corresponded to the monodentate interaction and the smallest Δ ($<110\text{ cm}^{-1}$) to the chelating bidentate. The medium range of Δ ($140\text{--}190\text{ cm}^{-1}$) was reported for bridging. In this study, the Δ ($1514\text{--}1373 = 141\text{ cm}^{-1}$) was ascribed as bridging bidentate. These results provide further support for VP intercalation into the interlay space of layered double hydroxides.

The comparisons between the FT-IR spectrum of MD-Zn/AI-LDH and various spectrum groups of LDH such as aromatic, carboxylic acid, methyl, and amidic are visible, indicating successful loading of drug in LDH (Figure 3). The peak of 3440 cm^{-1} is related to stretching vibrations of –OH group under the effect of hydrogen bond through water molecules and metal hydroxyl existing in hydroxide layers. Also, 472 cm^{-1} is related to the metal–oxygen group. Peak in 3743 cm^{-1} is related to stretching vibrations of N–H group of drug and peak of 1384 cm^{-1} and 1554 cm^{-1} to symmetrical and asymmetric stretching vibrations of the carboxylate group. The observed peak of 1628 cm^{-1} aromatic ring of methylodopa overlapped with hydroxyl groups.

Zeta potential of Zn/AI-LDH was measured at $+30\text{ mV}$ (data are not shown); the high superficial charge of LDH makes them easily stick to the negative surface of the cells to penetrate them.

Antibacterial and cytotoxicity assays

MTT assay was applied for the determination of the toxicity of nanoparticles based on the size and amount. The results showed that Zn/AI-LDH nanoparticles with a size of (200–300) nm have a less negative effect on C2C12 cells, and 94% of the cells were healthy compared to the control group (Figure 4(a)). Also, there was no significant difference

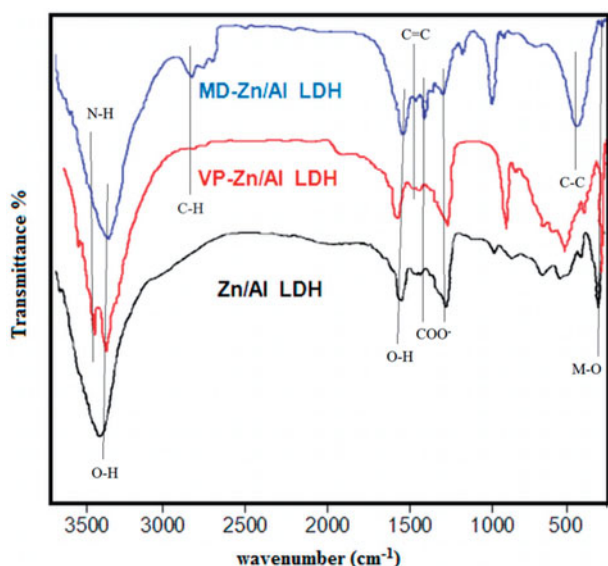


Figure 3. FT-IR spectra for (a), Zn/AI-LDH, (b) VP- Zn/AI-LDH, and (c) MD-Zn/AI-LDH.

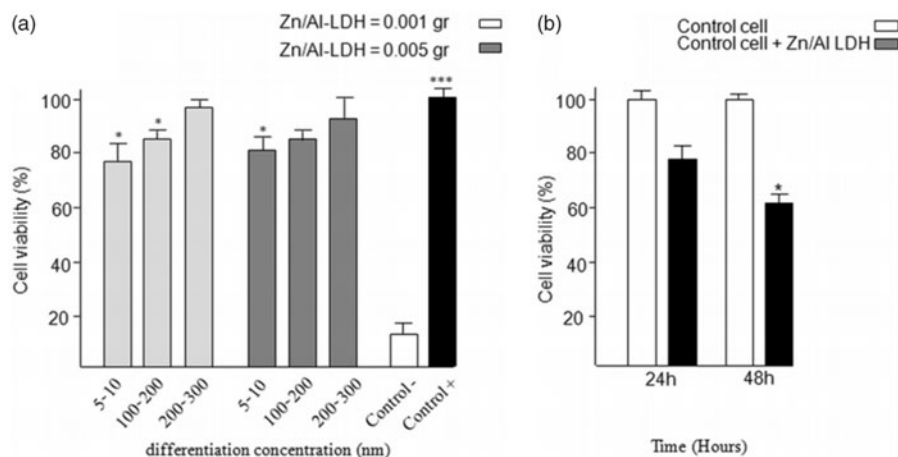


Figure 4. The result of MTT assay (a) for comparison between the particles with size of (5–10) nm, (50–100) nm, and (200–300) nm, in tow difference amount of nanoparticle consisting of 0.001 g and 0.005 g, (b) for antibacterial activity. The bacterial proliferation approximately decreases 30–40% in growth rate compared to that of the control cells.

between the two concentrations of nanoparticles (0.001 g and 0.005 g) on cell viability.

Moreover, the result of MTT assay for antibacterial activity demonstrated that bacterial proliferation approximately decreased by 30–40% in comparison to the control group (Figure 4(b)).

Loaded LDH destruction in acidic buffer with PH = 1.2 (simulated with the gastric environment)

Degradation of hydroxide layer in acidic buffer with PH = 1.2 (simulated with the gastric environment) prevents the performance of nanoparticles in drug delivery. Absorption spectra of solution buffer content of drug-loaded nanoparticles indicated that time has a central role. As shown in Figure 5, there was no destruction in the structure of the layers in the absence of the drug in the intervals between 75 to 27 min of the solution. After 90 min, drug concentration gradually began to elevate for the next 90 min in the solution to reach its maximum in the first 3 h.

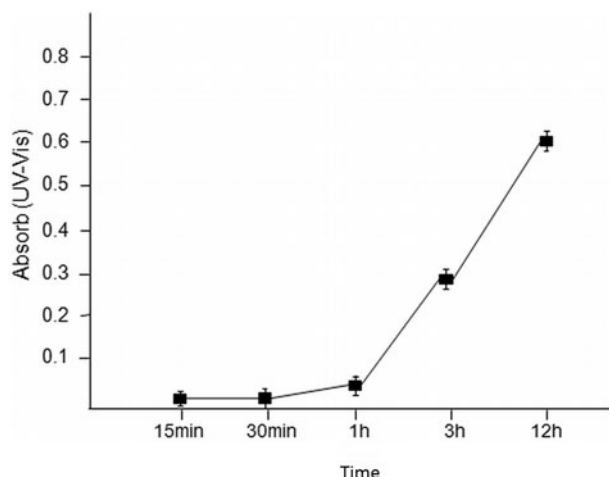


Figure 5. Correctness of the drug loaded by drug release in the phosphate buffer (pH = 7.4) solution and absorption via UV-Vis Spectrophotometer in specified intervals.

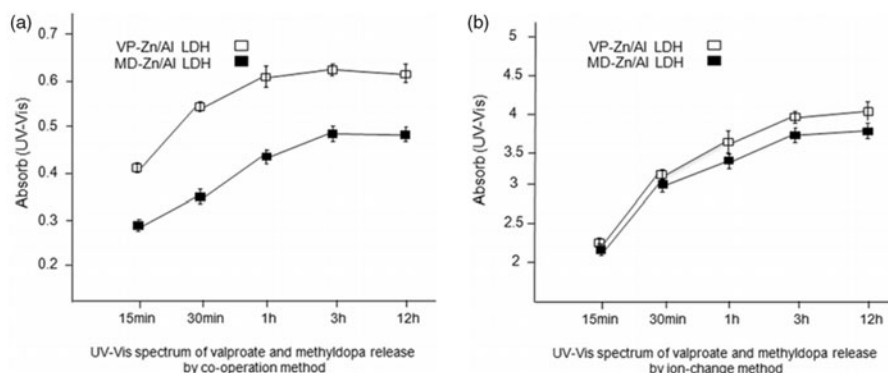


Figure 6. (a) UV-Vis spectrum of valproate and methyldopa release in intervals of 15 min, 30 min, 1 h, 3 h and 12 h in wavelength of 250 nm for valproate (VP) and 280 nm for methyldopa (MD) by co-operation method; (b) UV-Vis spectrum of valproate and methyldopa release in intervals of 15 min, 30 min, 1 h, 3 h and 12 h in wavelength of 250 nm for valproate (VP) and 280 nm for methyldopa (MD) by ion exchange method.

UV-Vis spectrum of valproate and methyldopa release assay

The correctness of the drug loading was determined by drug release in the phosphate buffer solution (pH = 7.4), and absorption was measured by UV-Vis spectrophotometer in specified intervals. According to Figure 6, a and b in both methods, drug release was determined in intervals of 15 min, 30 min, 1 h, 3 h, and 12 h in the wavelength of 250 nm for valproate and wavelength of 280 nm for methyldopa. Drug release gradually increased during 15 min to 1 h interval, and the concentration of drug was constant through 3 h to 12 h of interval. The results of drug loading and release indicated that co-operation greatly modulates the efficiency in comparison to ion exchange method.

Gene loading into Zn/Al-LDH correctness assay

Agarose gel electrophoresis was used for determination of the appropriate pCEP4/Cdk9 gene loading into the interlayer of LDH (Figure 7(a)). Cdk9 as the main core of PTEF-b complex for phosphorylation RNA polymerase (RNAP) is a therapeutic target for crucial diseases; particularly cancers [32]. Pure DNA (pCEP4/Cdk9) was observed in the gel, while the DNA complexed to the LDH samples (pCEP4/Cdk9 + Zn/Al-LDH) was not obvious, and no band was affected, indicating that pCEP4/Cdk9 was completely surrounded by Zn/Al-LDH nanoparticles.

Also, the concentration of pCEP4/Cdk9 was measured before and after the loading of the gene into the Zn/Al-LDH interlayer by UV-spect absorption in the wavelength of 260 nm. Observation of significant changes in the concentration of pCEP4/Cdk9 indicated high capacity of LDH nanoparticles in the absorption of DNA (Figure 7(b)).

Real-Time PCR and Western Blotting results of Cdk9 gene expression in transfected cells

The colonies of transfected C2C12 cells including pCEP4/Cdk9 + Zn/Al-LDH were harvested and processed for Real Time PCR assay (Figure 8(a)). Relative Cdk9 expression levels were analyzed, and the results indicated the over-expression

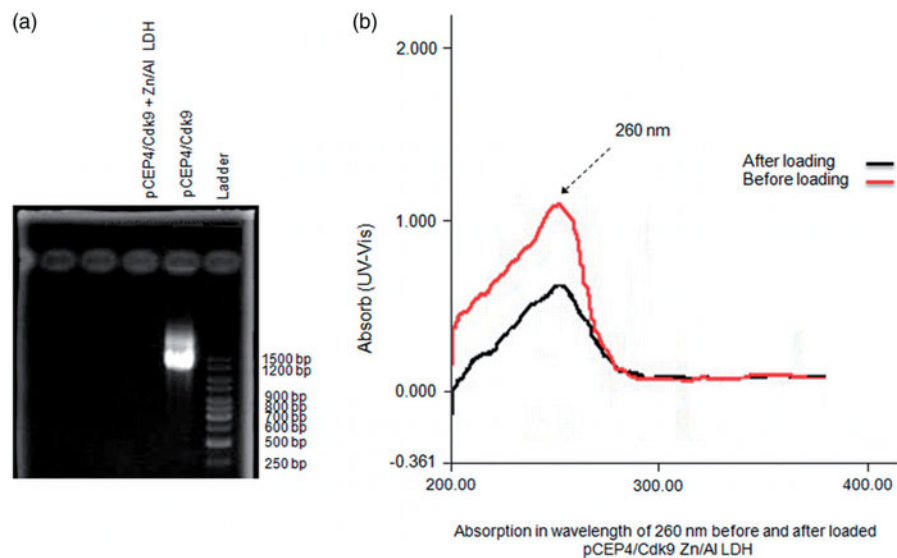


Figure 7. Zn/AI-LDH nanoparticles take up pCEP4/Cdk9 gene (a) Association/intercalation of pCEP4/Cdk9 with/in Zn/AI-LDH nanoparticles; Ladder, pCEP4/Cdk9-Zn/AI-LDH, and pCEP4/Cdk9 alone respectively. (b) Absorption in wavelength of 260 nm before and after loaded pCEP4/Cdk9 gene with/in Zn/AI-LDH.

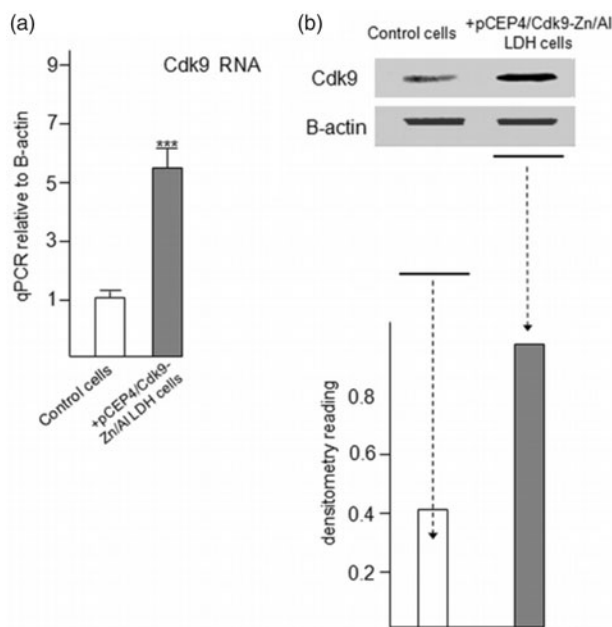


Figure 8. Increased expression of Cdk9 in C2C12 cells followed by taking up and releasing of pCEP4/Cdk9 gene with/in Zn/AI-LDH nanoparticle. (a) Increased Cdk9 expression in transfected C2C12 cells was analyzed by quantitative Real-Time PCR assay ($n=6$). (c) Cdk9 protein level in transfected and control cells was examined by Western blot analysis. (d) Data are expressed as mean \pm SEM *** $p < .001$

of Cdk9 in transfected colonies. Western blotting analysis showed that the level of Cdk9 dramatically increased in transfected colonies (Figure 8(b)). The results of Real-Time and Western Blotting of Cdk9 gene confirmed the potent ability of Zn/AI-LDH to load and in the delivery of the gene.

Conclusion

Zn/AI-LDH nanoparticles are a good candidate for drug/gene delivery systems due to their ease and inexpensive synthesis process. In the present study, Zn/AI-LDH nanoparticles were provided with the lateral size of 5–300 nm. The size of

nanoparticles plays an important role in drug/gene loading and release. Based on our results, the optimal size for effective drug/gene loading of Zn/AI-LDH nanoparticles is 30–100 nm.

Comparing two methods of co-operation and ion exchange in the loading of valproate and methyldopa showed that the co-operation method has a very high efficiency in both drug loading and drug release.

The positive zeta potential of 30 mV makes it very suitable for cellular uptake. The Zn/AI-LDH nanoparticle toxicity test shows that particles with sizes lower than 10 nm have a higher toxicity than particles with size of 30–50 nm. LDH's buffer capacity protects valproate and methyldopa from acidic environment of gastric and leads the drug to the exact activity location of it.

We used Zn/AI-LDH as Cdk9 gene carrier which was cloned in plasmid pCEP4 for gene expression enhancement in C2C12 cells. Zn/AI-LDH nanoparticles are able to bind to the plasmid tightly and facilitate their uptake into C2C12 cells. The test for plasmid delivery indicated that Zn/AI-LDH can be utilized as an effective carrier in gene delivery and gene therapy. The expression of Cdk9 increased in both RNA and protein level.

In conclusion, our results showed that the Zn/AI-LDH nanoparticles can function as useful tools for drug delivery and cellular uptaking of genes. Therefore, because of easy and inexpensive production of Zn/AI-LDH nanoparticles, they are suggested as proper and reliable alternatives to traditional and expensive methods such as Lipofectamine for gene delivery.

Ethical approval

All procedures performed in the study were in accordance with the ethical standards of the Ethics Committee at the Iran National Science Foundation (INSF) and with the 1964 Helsinki declaration and its later amendments or comparable ethical standards.

Disclosure statement

There are neither ethical nor financial conflicts of interest involved in the manuscript. The manuscript contains only original unpublished work and is not being submitted for publication elsewhere.

Funding

This work was supported by Molecular Medicine Research Center, Tabriz University of Medical Sciences, Tabriz, Iran and Department of Chemistry, Faculty of Science, University of Maragheh, Iran.

ORCID

Vahid Yousefi  <http://orcid.org/0000-0002-9304-113X>

References

- [1] Kura AU, Hussein MZ, Fakurazi S, et al. Layered double hydroxide nanocomposite for drug delivery systems; bio-distribution, toxicity and drug activity enhancement. *Chem Cen J*. 2014;8:47.
- [2] Rives V, del Arco M, Martín C. Intercalation of drugs in layered double hydroxides and their controlled release: a review. *App Clay Sci*. 2014;88:239–269.
- [3] Hussein MZ, Ali SH, Zainal Z, et al. Development of antiproliferative nanohybrid compound with controlled release property using ellagic acid as the active agent. *Int J Nanomed*. 2011;6:1373.
- [4] Ladewig K, Niebert M, Xu ZP, et al. Controlled preparation of layered double hydroxide nanoparticles and their application as gene delivery vehicles. *App Clay Sci*. 2010;48:280–289.
- [5] Tyner KM, Schiffman SR, Giannelis EP. Nanobiohybrids as delivery vehicles for camptothecin. *J Control Release*. 2004;95:501–514.
- [6] Kuthati Y, Kankala RK, Lee C-H. Layered double hydroxide nanoparticles for biomedical applications: current status and recent prospects. *App Clay Sci*. 2015;112:100–116.
- [7] Li B, He J, Evans DG, et al. Inorganic layered double hydroxides as a drug delivery system—intercalation and in vitro release of fenbufen. *App Clay Sci*. 2004;27:199–207.
- [8] Gu Z, Rolfe BE, Thomas AC, et al. Cellular trafficking of low molecular weight heparin incorporated in layered double hydroxide nanoparticles in rat vascular smooth muscle cells. *Biomaterials*. 2011;32:7234–7240.
- [9] Wong Y, Markham K, Xu ZP, et al. Efficient delivery of siRNA to cortical neurons using layered double hydroxide nanoparticles. *Biomaterials*. 2010;31:8770–8779.
- [10] Xu ZP, Stevenson GS, Lu C-Q, et al. Stable suspension of layered double hydroxide nanoparticles in aqueous solution. *J Am Chem Soc*. 2006;128:36–37.
- [11] Xu ZP, Walker TL, Liu K-I, et al. Layered double hydroxide nanoparticles as cellular delivery vectors of supercoiled plasmid DNA. *Int J Nanomed*. 2007;2:163.
- [12] Xu ZP, Niebert M, Porazik K, et al. Subcellular compartment targeting of layered double hydroxide nanoparticles. *J Control Release*. 2008;130:86–94.
- [13] Choy J-H, Park M, Oh J-M. Gene and drug delivery system with soluble inorganic carriers. In: *NanoBioTechnology: bioInspired devices and materials of the future*. Humana Press: Springer; 2008. p.349–367.
- [14] Ali SA, Al-Qubaisi M, Hussein MZ, et al. Preparation of hippurate-zinc layered hydroxide nanohybrid and its synergistic effect with tamoxifen on HepG2 cell lines. *Int J Nanomed*. 2011;6:3099.
- [15] Gasser M. Inorganic layered double hydroxides as ascorbic acid (vitamin c) delivery system—Intercalation and their controlled release properties. *Coll and Surf B: Biointer*. 2009;73:103–109.
- [16] Badrzadeh F, Rahmati-Yamchi M, Badrzadeh K, et al. Drug delivery and nanodetection in lung cancer. *Artif Cells Nanomed Biotechnol*. 2016;44:618–634.
- [17] Rives V, del Arco M, Martín C. Layered double hydroxides as drug carriers and for controlled release of non-steroidal antiinflammatory drugs (NSAIDs): a review. *J Control Release*. 2013;169:28–39.
- [18] Rojas R, Palena M, Jimenez-Kairuz A, et al. Modeling drug release from a layered double hydroxide–ibuprofen complex. *App Clay Sci*. 2012;62:15–20.
- [19] Chen M, Cooper HM, Zhou JZ, et al. Reduction in the size of layered double hydroxide nanoparticles enhances the efficiency of siRNA delivery. *J Colloid Interface Sci*. 2013;390:275–281.
- [20] Choy J-H, Jung J-S, Oh J-M, et al. Layered double hydroxide as an efficient drug reservoir for folate derivatives. *Biomaterials*. 2004;25:3059–3064.
- [21] Jaubertie C, Holgado M, San Roman M, et al. Structural characterization and delamination of lactate-intercalated Zn, Al-layered double hydroxides. *Chem Mater*. 2006;18:3114–3121.
- [22] Ladewig K, Niebert M, Xu ZP, et al. Efficient siRNA delivery to mammalian cells using layered double hydroxide nanoparticles. *Biomaterials*. 2010;31:1821–1829.
- [23] San Román M, Holgado M, Jaubertie C, et al. Synthesis, characterisation and delamination behaviour of lactate-intercalated Mg, Al-hydroxalcite-like compounds. *Solid State Sci*. 2008;10:1333–1341.
- [24] Tarhriz V, Wagner KD, Masoumi Z, et al. CDK9 regulates apoptosis of myoblast cells by modulation of microRNA-1 expression. *J Cell Biochem*. 2018;119(1):547–554.
- [25] Lu Y, Wang L, Preuß K, et al. Halloysite-derived nitrogen doped carbon electrocatalysts for anion exchange membrane fuel cells. *J Power Sources*. 2017;372:82–90.
- [26] Sun X, Neuperger E, Dey SK. Insights into the synthesis of layered double hydroxide (LDH) nanoparticles: part 1. Optimization and controlled synthesis of chloride-intercalated LDH. *J Colloid Interface Sci*. 2015;459:264–272.
- [27] Mahjoubi FZ, Khalidi A, Abdennouri M, et al. Zn–Al layered double hydroxides intercalated with carbonate, nitrate, chloride and sulphate ions: synthesis, characterisation and dye removal properties. *J Taibah Univ for Sci*. 2017;11:90–100.
- [28] Eyvazi S, Kazemi B, Bandehpour M, et al. Identification of a novel single chain fragment variable antibody targeting CD24-expressing cancer cells. *Immunol Lett*. 2017;190:240–246.
- [29] Ren Y, Iimura K-i, Kato T. Structure of barium stearate films at the air/water interface investigated by polarization modulation infrared spectroscopy and π –A isotherms. *Langmuir*. 2001;17:2688–2693.
- [30] Zhang L, He R, Gu H-C. Oleic acid coating on the monodisperse magnetite nanoparticles. *Appl Surf Sci*. 2006;253:2611–2617.
- [31] Ukishima S, Iijima M, Sato M, et al. Heat resistant polyimide films with low dielectric constant by vapor deposition polymerization. *Thin Solid Films*. 1997;308:475–479.
- [32] Eyvazi S, Hejazi M, Kahroba H, et al. Cdk9 as an appealing target for therapeutic interventions. *Curr Drug Targets*. 2018;in-press.